Conf 8112 378 2

LA-UR -81-1875

TITLE: COSMIC-RAY-PRODUCED STABLE NUCLIDES: VARIOUS PRODUCTION RATES AND THEIR IMPLICATIONS.

AUTHOR(S): ROBERT C. REEDY

MASTER

SUBMITTED TO: PROCEEDINGS OF THE 12th LUNAR AND PLANETARY SCIENCE CONFERENCE.

University of California

LOS ALAMOS SCIENTIFIC LABORATORY
Post Office Box 1663 Los Alamos, New Mexico 87545
An Affirmative Action/Equal Opportunity Employer

Form No. 836 R3
St. No. 2629
12/78

UNITED STATES
DEPARTMENT OF ENERGY
CONTRACT W-7405-ENG. 36

COSMIC-RAY-PRODUCED STABLE NUCLIDES:
VARIOUS PRODUCTION RATES AND THEIR IMPLICATIONS

Robert C. Reedy

Nuclear Chemistry Group, Mail Stop 514
Los Alamos National Laboratory
Los Alamos, New Mexico 87545

15 June 1981

ABSTRACT

The rates for a number of reactions producing certain stable nuclides, such as ^{3}He and ^{4}He, and fission in the moon are calculated for galactic-cosmic-ray particles and for solar protons. Solar-proton-induced reactions with bromine usually are not an important source of cosmogenic Kr isotopes. The $^{130}Ba(n,p)$ reaction cannot account for the undercalculation of ^{130}Xe production rates. Calculated production rates of ^{15}N, ^{13}C, and ^{2}H agree fairly well with rates inferred from measured excesses of these isotopes in samples with long exposure ages. Cosmic-ray-induced fission of U and Th can produce significant amounts of fission tracks and of ^{86}Kr, ^{134}Xe, and ^{136}Xe, especially in samples with long exposures to cosmic-ray particles.

INTRODUCTION

Cosmic-ray-induced reactions in extraterrestrial matter are important sources of certain stable nuclides, such as the noble gases (Hohenberg et al., 1978) and ^{15}N (Becker et al., 1976). Cosmic-ray-induced reactions with uranium and thorium could produce a significant fraction of the fissions observed in certain samples (Woolum and Burnett, 1974; Damm et al., 1978), and cosmogenic fissions might be an important source of certain nuclides, such as ^{86}Kr and ^{136}Xe (Regnier, 1977). These stable products of cosmic-ray reactions in extraterrestrial matter are important both for studies of the exposure of samples to cosmic rays and for corrections which must be applied to raw data to deduce other "components" (e.g., "trapped" noble gases).

Calculated production rates for neon, argon, krypton, and xenon were reported and compared with observed results by Hohenberg et al. (1978). Improved krypton calculations and comparisons were given by Regnier et al. (1979). Calculated production rates for several noble-gas nuclides (e.g., ^{130}Xe) did not agree well with rates inferred from observed data and certain target elements (bromine, thorium, and uranium) were not included. The reaction $^{130}Ba(n,p)$ is studied here to see if it could improve the agreement of calculated and observed ^{130}Xe concentrations. The possible importance of solar-proton reactions with bromine in producing Kr isotopes is examined. Cosmogenic fission is considered as sources of ^{86}Kr, ^{134}Xe, and ^{136}Xe. Rates for a number of cosmogenic reactions have not been calculated (e.g., ^{13}C) or reported (e.g., He) previously. Reported here are the rates for producing ^{3}He, ^{4}He, ^{15}O (which decays to ^{15}N), ^{13}C, and ^{2}H and for the cosmogenic fission of thorium and uranium by energetic cosmic-ray particles (including the production of ^{86}Kr, ^{134}Xe, and ^{136}Xe).

Reactions induced by both galactic-cosmic-ray (GCR) particles and solar protons are considered for most products. The lunar particle fluxes of Reedy and Arnold (1972) were used. Two spectral parameters for solar protons

(R_0 = 100 and 200 MV) were used with the exponential-rigidity expression, $dJ/dR = K \exp(-R/R_0)$, for proton flux J. In lunar samples, most radionuclides have been produced by solar protons which had a spectral shape with R_0 = 100 MV (e.g., ^{26}Al and ^{53}Mn; Kohl et al., 1978). However, the spectral shape of solar protons producing 2.1×10^5-year ^{81}Kr appears to have been much harder (Reedy, 1980), hence the inclusion of rates for a spectral parameter of R_0 = 200 MV. An omnidirectional (4π) flux of 100 protons/cm^2 s for protons with E > 10 MeV was adopted. The actual fluxes of solar protons during various time periods have varied considerably about this adopted flux (Reedy, 1980). Wherever possible, experimental excitation functions - cross sections as a function of energy - were used; otherwise, excitation functions were estimated from cross sections for analogous reactions or by theoretical systematics. Production rates for making ^{22}Ne from Mg calculated with the new excitation functions of Reedy et al. (1979) agreed within 1% with those reported earlier by Hohenberg et al. (1978).

HELIUM

Rates for the GCR and solar-proton production of ^3He and ^4He were not reported in Hohenberg et al. (1978) because there were no good observed He data with which to make comparisons. There appear to have been significant (~30%) diffusion losses of Ne in lunar samples (Hohenberg et al., 1978), and diffusion losses of He are expected to be much larger. Yaniv et al. (1981) reported retention of only ≈1% of cosmogenic ^3He in the top centimeter of lunar rock 65315. They also noted that an observed excess of ^3He above that expected from cosmic-ray-induced reactions in the top millimeter was evidence for solar-flare-implanted ^3He. Rao and Venkatesan (1980) and Venkatesan et al. (1980) observed that the ratios of cosmogenic ^3He to cosmogenic ^{21}Ne varied over narrow ranges in several samples of rocks 61016 and 66435 and that the solar-proton exposure ages for ^3He agreed with the ^{21}Ne and ^{38}Ar exposure ages, and concluded that there was no significant depth-dependent diffusion in their samples. Cosmogenic helium generally is retained in meteorites, and ^3He is often used in studies of cosmic-ray exposure ages (see, e.g., Cressy and Bogard, 1976). Meteorite data will be used below in comparing observed and calculated ^3He production rates.

Excitation functions were compiled for the production of ^3He and ^4He from the major target elements (oxygen, magnesium, aluminum, silicon, and iron). The excitation functions in Reedy and Arnold (1972) for the production of ^3H (which decays to ^3He) were used. For the direct production of ^3He from oxygen by both GCR particles and protons, the excitation function was assumed to have the shape of that for producing ^3H from oxygen and was normalized to the experimental cross sections at 600 and 3000 MeV of Kruger and Heymann (1973). For the direct production of ^3He from Mg, Al, and Si by protons, the measured cross sections of Walton et al. (1976a), Goebel et al. (1964), and Kruger and Heymann (1973) were used. The excitation functions for the production of ^3He by GCR-produced neutrons were the same as for the protons, but with the energies below ≅30 MeV raised by 2 or 3 MeV for Al or lowered by 3 or 4 MeV for Si to correct for differences in threshold energies for the neutron- and proton-induced reactions. For the GCR-particle and proton production of ^3He from Fe, the experimental data above 150 MeV that were compiled by Goebel et al. (1964) were used; estimated cross sections were used at lower energies. The adopted cross section near 30 MeV are similar to the Ni(p,x)^3He cross sections measured by Pulfer (1979).

For the proton production of ^4He from these elements, experimental cross sections from the same references cited above for ^3He were used. For iron and protons with $E < 20$ MeV, the measured (p,α) cross sections of Kumabe et al. (1963) and Sherr and Brady (1961) and the shape of the (p,α) excitation function of Fulmer and Goldman (1960) were used. For the production of ^4He by GCR particles with oxygen, the threshold energy was lowered from 8 MeV to 4 MeV. For GCR production of ^4He from Mg, Al, and Si for $E < 10$ MeV, the $^{27}Al(n,\alpha)^{24}Na$ excitation function (see compilation of Garber and Kinsey, 1976) was used. Similarly, the

$^{54}Fe(n,\alpha)^{51}Cr$ excitation function was used for ^{4}He production from Fe by GCR secondary neutrons with $E < 10$ MeV.

The calculated production rates of ^{3}He (including ^{3}H decay) and ^{4}He are given in Table 1 for GCR particles and in Tables 2 and 3 for solar protons with spectral shapes having $R_0 = 100$ and 200 MV, respectively. Solar-proton production rates also were calculated using spectrum A of Walton et al. (1976b), which has a shape of $dJ/dE = K\,E^{-2.55}$. For depths within 1 g/cm^2 of the surface, the calculated results generally agreed with those of Walton et al. (1976b) within 10%. At greater depths, the calculated rates of Walton et al. (1976b) were much lower than those calculated here (by a factor of ~2 at 20 g/cm^2); the disagreement was due mainly to the fact that Walton et al. (1976b) ignored protons with $E >$ 200 MeV, whereas this work considered all energies with $E < 3668$ MeV.

Of the total GCR production of ^{3}He, slightly less than 0.5 was calculated as being due to the production and decay of ^{3}H. For solar-proton-induced reactions, approximately 0.4 of the ^{3}He is made by way of ^{3}H. In lunar samples, Reedy (1977) found that the measured ^{3}H activities at deep depths were about 1.4 times the calculated GCR production rates. There are no good experimental data for comparing observed and calculated production rates of ^{3}H in meteorites or of ^{3}He in lunar samples. For the Keyes and St. Séverin chondrites, the calculated ^{3}He exposure ages were 1.3-1.4 times those calculated using ^{21}Ne and ^{38}Ar data (Reedy et al., 1978; Reedy et al., 1979). Because the calculated ^{21}Ne production rates of Reedy et al. (1979) agree fairly well with those determined from ^{53}Mn exposure ages (Nishiizumi et al., 1980; Müller et al., 1981), this factor of 1.3-1.4 probably applies also to the observed/calculated ^{3}He production rates. Thus, both lunar ^{3}H data and meteoritic noble-gas data imply that the calculated GCR production rates for ^{3}He should be multiplied by $\cong$1.4 to get actual ^{3}He production rates. Because oxygen produces $\cong$0.6 of the total ^{3}He and because production cross sections of ^{3}He from oxygen are not known well, this observed/calculated ratio of ≅1.4 probably results from the $O(p,x)^3He$ cross sections used here being too low.

Most of the ^4He in extraterrestrial samples is radiogenic, being produced by the alpha decay of U and Th and their daughter isotopes. Using the meteoritic particle fluxes of Reedy _et al._ (1979), a $^4He/^3He$ production ratio of about 7 was calculated. Using the ^3He normalization factor of 1.4 given above, the predicted cosmogenic $^4He/^3He$ production ratio is about 5, the same number that Signer and Schultz (1976) used to correct measured ^4He concentrations for cosmogenic ^4He. In iron meteorites, almost all of the observed ^4He is produced by cosmic-ray-induced reactions with Fe. The measured $^3He/^4He$ ratios in iron meteorites are usually 0.22-0.28 (Signer and Nier, 1962), much larger than the production ratios calculated here for Fe (0.07-0.19), or the cross-section ratios measured at 600 and 2000 MeV (about 0.15, Goebel _et al._, 1964).

SOLAR-PROTON PRODUCTION OF KRYPTON ISOTOPES FROM BROMINE

Production rates of krypton isotopes by cosmic-ray particles have been calculated previously (Regnier _et al._, 1979) for the target elements rubidium, strontium, yttrium, and zirconium, and for neutron-capture reactions with bromine. Because of the recent use of ^{81}Kr to study solar-proton fluxes over the last ≅3 x 10^5 years (Reedy, 1980), some production-rate calculations were made to see whether reactions with bromine, like $^{81}Br(p,n)^{81}Kr$, could be important in producing Kr isotopes in the surface layers of lunar rocks. Excitation functions for the $^{81}Br(p,n)^{81}Kr$, $^{81}Br(p,2n)^{80}Kr$, $^{81}Br(p,pn)^{80}Br$, $^{81}Br(p,4n)^{78}Kr$, and $^{79}Br(p,2n)^{78}Kr$ reactions were constructed using analogous reactions with ^{89}Y (Birattari _et al._, 1973), ^{79}Br (Collé and Kishore, 1974), and other odd-even nuclei in this A ~ 80 mass region. All but the (p,4n) cross sections are probably well estimated because most analogous reactions had similar excitation functions after correcting for differences in threshold energies. Tables 2 and 3 give the calculated ^{81}Kr, ^{80}Kr, and ^{78}Kr production rates from bromine for several depths using solar protons with R_o = 100 and 200 MV spectral shapes, respectively.

For ^{81}Kr, solar-proton-induced reactions with bromine contributed very little, being most important for the surface layers (≅5% for the top 0.5 mm of lunar rock 68815). This calculated contribution is probably an upper limit as most of the ^{82}Kr and ^{80}Kr produced by neutron-capture reactions with Br are not retained in lunar rocks (Regnier et al., 1979). Bromine was most important for ^{78}Kr at the surface, where ≅40% of the calculated solar-proton production was from Br. However, most of ^{78}Kr, even at the surface, is made by galactic-cosmic-ray particles. Therefore production of Kr isotopes from Br should be unimportant unless a sample has a very high abundance of Br or, for ^{81}Kr, unless there were many more protons with energies between 2 and 10 MeV than observed recently via the ^{56}Fe(p,n)^{56}Co reaction. (Protons with energies below 10 MeV cannot produce ^{26}Al, ^{53}Mn, and most other long-lived radionuclides, so there is no way to detect their presence in the past by these cosmogenic radionuclides.)

PRODUCTION OF ^{130}Xe BY THE ^{130}Ba(n,p) REACTION

Kaiser (1977) measured the proton-induced cross sections for the production of Xe isotopes from natural barium. Production rates calculated using his cross sections have matched most measured Xe isotopic ratios. However the ^{130}Xe/^{126}Xe ratio is undercalculated by ≅40% (Hohenberg et al., 1978). Kaiser (1977) and Hohenberg et al. (1978) felt that the deficiency in calculating ^{130}Xe production rates may have been the omission of neutron-induced reactions, specifically ^{130}Ba(n,p). Neutron-deficient isotopes of an element have larger (n,p) cross sections than the isotopes with higher masses, so a large ^{130}Ba(n,p) cross section is possible even though ^{136}Ba and ^{138}Ba have (n,p) cross sections of only a few millibarns (Garber and Kinsey, 1976).

To see quantitatively how important the ^{130}Ba(n,p) reaction could be in calculating ^{130}Xe production rates from barium, an excitation function for that reaction was constructed using a shape obtained from other (n,p) reactions in the A ~130 mass region and assuming a peak cross section of 0.5 barns at 20 MeV. (Kaiser [1977] has estimated that the ^{130}Ba(n,p) reaction might have a peak cross section of ~0.55 b at an energy of 25 MeV.) Calculated production rates of ^{130}Xe via the ^{130}Ba(n,p) reaction were 0.002 to 0.02 of those calculated via the Ba(p,x)^{130}Xe excitation function of Kaiser (1977). The reason that the ^{130}Ba(n,p) contributes so little is that only 0.11% of the isotopes of natural barium are ^{130}Ba, so a 0.5-barn cross section for ^{130}Ba is only about 0.5 mb for natural barium. Kaiser (1977) measured a 0.39 mb cross section for 38-MeV protons producing ^{130}Xe and a peak Ba(p,x)^{130}Xe cross section of 31.5 mb at 300 MeV.

These calculated ^{130}Ba(n,p)/Ba(p,x)^{130}Xe production ratios show that the majority of ^{130}Xe production from Ba via galactic-cosmic-ray particles is by spallation reactions with protons having energies above ~100 MeV. The ^{130}Ba(n,p) reaction should not have a cross section which is considerably greater than 0.5 b because the total nonelastic cross section is 2 b (Garber and Kinsey, 1976), so this reaction should not be an important source of cosmogenic ^{130}Xe. Kaiser and Berman (1972) irradiated natural barium with neutrons having a continuum of energies below about 30 MeV and did not see any ^{130}Xe above their blank levels, while they saw large amounts of ^{131}Xe made by the ^{130}Ba(n,γ) reaction. Eberhardt et al. (1971) didn't observe any ^{130}Xe in a sample of Ba-feldspar irradiated in a reactor with epithermal and fast neutrons. Thus the cause of the undercalculation of ^{130}Xe production rates by Hohenberg et al. (1978) and Kaiser (1977) is not known.

NITROGEN-15 (OXYGEN-15)

In a number of lunar samples, there is a ^{15}N-rich component of nitrogen which is released at high temperatures and which is made by cosmic-ray-induced spallation reactions (Becker et al., 1976). To calculate production-rate-versus-depth profiles for ^{15}N, the $^{16}O(p,pn)^{15}O$ cross sections compiled by Audouze et al. (1967) were adopted. The ^{15}O-production cross sections were used because there are very few cross sections for the direct production of ^{15}N, and both nuclides are produced by similar reactions. The calculated ^{15}O production rates are given in Tables 1, 2, and 3.

The only measured $^{16}O(n,2n)^{15}O$ cross sections (Brill' et al., 1961) have a maximum of 16 mb (±30%) at 31 MeV, while the $^{16}O(p,pn)^{15}O$ cross sections used here were 30 mb at 30 MeV and 74 mb at 55 MeV. An excitation function for the production of ^{15}O by GCR particles was constructed using these (n,2n) cross sections at low energies (mainly $E < 100$ MeV) and the (p,pn) cross sections at high energies. The production rates calculated with the (p,pn) cross-section set were from 1.9 (at the lunar surface) to 3.15 (for depths >500 g/cm^2) of those calculated with the GCR cross-section set. The shape of an excitation function determines the production-rate profile as a function of depth (Reedy and Arnold, 1972). The excitation function which really should be used for ^{15}N production from ^{16}O should include the sum of the (n,2n), (n,d), (n,np), (n,pn), and (n,2p) cross sections for neutron-induced reactions and the sum of the (p,pn), (p,np), and (p,2p) cross sections for proton-induced reactions. (All of these reactions with ^{16}O produce mass-15 nuclides, including ^{15}O and ^{15}C which rapidly decay to ^{15}N.) The choice of which of the two excitations functions to use for ^{15}N production was based on which shape was most similar to the shape of the excitation function which really should be used. Because the ^{16}O $(p,pn)^{15}O$

excitation function has a shape which probably is the better approximation of the desired shape, it was used here.

In their studies of cosmogenic ^{15}N in lunar samples with known exposure ages, Becker et al. (1976) empirically determined a ^{15}N production rate of 3.6 (±0.8) pg ^{15}N/g/m.y., which is equivalent to 275 atoms/min/kg. This production rate is 1.55 times greater than the calculated rate in Table 1 for ^{15}O at 5 g/cm^2, assuming an oxygen abundance of 0.435. This factor of 0.55 for direct ^{15}N production relative to ^{15}O production seems low, but is not an unreasonable value, given both experimental and calculational uncertainties. The empirical production rate of Becker et al. (1976) could be low because some cosmogenic ^{15}N might be released at low temperatures. As noted above, there also are uncertainties in the production cross sections for ^{15}O and ^{15}N. The excitation function which used $^{16}O(n,2n)^{15}O$ cross sections at low energies gave a calculated production rate at a depth of 5 g/cm^2 which was 0.50 of that given in Table 1, so the empirical/calculated production-rate ratio of 1.55 would become 3.1.

In the atmospheres of Mars and Earth, the $^{14}N/^{15}N$ ratios are 165 and 277, respectively (Owens et al., 1977). Assuming that nitrogen in the Earth's atmosphere is typical of solar-system nitrogen, the martian atmosphere has a ^{15}N excess of $\cong 6 \times 10^{19}$ atoms/cm^2. This enrichment in ^{15}N usually is considered to have resulted from isotopic fractionation when large amounts of atmosphere escaped from Mars. An excess of ^{15}N also could be produced by cosmic-ray-induced reactions with oxygen atoms in the martian atmosphere or surface. When the lunar ^{15}O production rates are integrated over all depths, an oxygen abundance of 45% is assumed, and the factor of 1.55 is used to convert to total ^{15}N production, the total GCR and R_0 = 100 MV solar-proton production rates are 89 and 7 atoms/min/cm^2, respectively. Over 4.5×10^9 years, the production of cosmogenic ^{15}N is 2.3×10^{17} atoms/cm^2, slightly less than 0.5% of the observed excess of ^{15}N in the martian atmosphere. Yanagita and Imamura (1978), using simpler calculations, also have concluded that contemporary cosmic-ray fluxes could not produce this excess ^{15}N in the martian atmosphere.

CARBON-13

Like ^{15}N, ^{13}C also is enriched in the high-temperature fractions from lunar samples and the amount of the enrichment is proportional to the sample's exposure age (Des Marais, 1980). Using the Monte Carlo calculations of Armstrong and Alsmiller (1971) for the production rates of ^{15}N and ^{13}C, Des Marais (1978) estimated a $^{13}C/^{15}N$ production ratio of approximately 0.32. If all the production rates of mass-13 and mass-15 isobars in Fig. 2 of Armstrong and Alsmiller (1971) are summed, then a net $^{13}C/^{15}N$ production ratio of about 0.30 is obtained. Shapiro and Silberberg (1970) give $^{13}C/^{15}N$ production ratios from oxygen of 0.40 to 0.48 for protons with E = 150 and ≧2300 MeV, respectively. To check the $^{13}C/^{15}N$ production ratio, excitation functions for the cumulative production of ^{13}C (including ^{13}N, which decays to ^{13}C) were prepared.

For protons with E < 50 MeV, the experimental cross sections for the $^{16}O(p,x)^{13}N$ reaction of Albouy et al. (1962) were used. The peak $^{16}O(p,\alpha)^{13}N$ cross section is 19 mb for E = 19-25 MeV. For neutrons with E < 20 MeV, the $^{16}O(n,\alpha)^{13}C$ cross sections evaluated by Foster and Young (1972) were adopted. Peak cross sections for the $^{16}O(n,\alpha)^{13}C$ reactions were 120 mb for E ≅ 5 MeV and ≅200 mb near 10 MeV. Above 50 MeV, there are only data for ^{13}N production, the cross sections being ≅5 mb from E ≅ 80 MeV to E = 5.7 GeV (Audouze et al., 1967). Armstrong and Alsmiller (1971) calculated that the $^{13}C/^{13}N$ production ratio was about 5, which would imply a ^{13}C + ^{13}N production cross section of ≅30 mb. Shapiro and Silberberg (1970) calculated total ^{13}C production cross sections from oxygen of 20-25 mb for E > 150 MeV. For E > 75 MeV, the average of these cross sections, 25 mb, was adopted. The $^{16}O(p,pn)^{15}O$ cross sections are greater than those for

^{13}C production from 25 to ≅2500 MeV, but lower than the $^{16}O(p,\alpha)^{13}N$ or $^{16}O(n,\alpha)^{13}C$ cross sections below 25 MeV. The production rates for ^{13}C from oxygen are given in Table 1 for GCR reactions and Tables 2 and 3 for solar protons.

The $^{13}C/^{15}O$ production ratios calculated for GCR particles ranged from 0.98 at the surface to 2.13 below 500 g/cm^2. Assuming a $^{15}N/^{15}O$ production ratio of 1.55 (see above), the $^{13}C/^{15}N$ GCR production ratios would range from 0.63 to 1.38. The $^{13}C/^{15}N$ production ratio is calculated to be 1.0 at 65 g/cm^2. The $^{16}O(n,\alpha)^{13}C$ reaction, which has large cross sections, is the main reason that the $^{13}C/^{15}N$ production ratio is much higher than predicted by Shapiro and Silberberg (1970) for reactions by high-energy protons. Because Armstrong and Alsmiller (1971) included low-energy neutrons in their calculations, it is not clear why their $^{13}C/^{15}N$ production ratio is a factor of ~3 below those calculated here.

The largest ^{13}C enrichment observed by Des Marais (1980) was for lunar rock 15499. Assuming this rock's excess ^{13}C corresponded to a $\delta^{13}C$ of 75 per mil, that its exposure age (in 10^6 years) divided by its C abundance (in μg/g) was 480, and its oxygen abundance was 0.435, the observed production rate of ^{13}C in 15499 was ≅380 atoms/min/kg(O). This ^{13}C production rate is comparable to, but somewhat smaller than, those given in Table 1. As with ^{15}O, there are uncertainties in both the observed and calculated ^{13}C production rate. About 65% of the ^{13}C is calculated to have been produced by particles with E > 30 MeV and, as noted above, there are considerable uncertainties in the cross sections for ^{13}C production from oxygen at such energies.

The amount of excess ^{13}C observed by Des Marais (1980) is consistent with the production rates calculated here. Spallogenic ^{13}C usually will be harder to detect than spallogenic ^{15}N because (1) the average $^{13}C/^{15}N$ production rate is <1 for most samples, (2) the carbon content of most samples is much higher than their nitrogen content, and (3) ^{13}C is 1.11% of natural carbon, while ^{15}N is only 0.37% of normal nitrogen.

DEUTERIUM

The heavy isotope of hydrogen, deuterium (^2H), like ^{13}C and ^{15}N, is found normally in low abundances in most lunar materials. Because the $^2H/H$ ratio in the solar wind is expected to be very low (see, e.g., Epstein and Taylor, 1971), the relatively high ^2H contents of lunar samples were recognized by Epstein and Taylor (1971) and Friedman et al. (1971) to be due to deuterium production by spallation reactions. Merlivat et al. (1974) made a rough estimation of the production rate of deuterium on the lunar surface. Merlivat et al. (1976) measured the deuterium content of eight samples in 70215, including five with a distribution of known depths, and determined a production rate of 0.46 x 10^{-10} mole $^2H_2/g/10^8$ years (1050 atoms/min/kg). They didn't see any variation in spallogenic ^2H content with sample depth, a trend consistent with the rock's long, complex exposure history. Merlivat et al. (1976) reported unpublished deuterium production rates calculated by Yokoyama and Tobailem of about 1030 and 1010 atoms/min/kg at 4 and 8 cm, respectively, for an erosion rate of 0.5 mm/10^6 years, and noted that their inferred ^2H production rate was about 4.6 times the measured tritium (^3H) activities in other lunar samples.

There are very few measured cross sections for the production of deuterium, so the excitation functions used here in calculating production rates have considerable uncertainties. For the major target element oxygen, the evaluated $^{16}O(n,d)$ cross sections of Foster and Young (1972) were used for GCR particles with E < 15 MeV. For proton-induced reactions, the energies for these cross sections were raised by 4 MeV to account for the different threshold energies. At 39 and 62 MeV, the experimental $^{16}O(p,x)^2H$ cross sections of Bertrand and Peelle (1973) were used. At 300 and 600 MeV, the tritium cross sections of Reedy and Arnold (1972) times the $^2H/^3H$ production ratio of 9.1 reported by Badhwar and Daniel (1963) for 300-MeV protons reacting with oxygen were adopted.

Badhwar and Daniel (1963) also reported that 190-MeV protons reacting with Al and Ni had $^{2}H/^{3}H$ production ratios 5.6 and 4.7, respectively. Similar $^{2}H/^{3}H$ production ratios were measured by Bertrand and Peelle (1973) for 62 MeV protons reacting with Al and Fe. For the cross sections for ^{2}H production from Mg, Al, Si, and Fe by both GCR particles and protons, the tritium cross sections of Reedy and Arnold (1972) were multiplied by 6, 6, 6, and 5, respectively, and the energies for the reaction thresholds were lowered. The calculated deuterium productions from these five target elements are given in Table 1 for GCR particles and in Tables 2 and 3 for solar protons.

In the top 40 g/cm^2 of a lunar rock, the GCR production rate of deuterium would be about 1200 atoms/min/kg, in quite good agreement with the inferred and calculated values reported in Merlivat et al. (1976). In lunar samples, ≅70-80% of the ^{2}H is calculated as having been produced from reactions with oxygen. Within 100 g/cm^2 of the moon's surface ≅80-95% of the GCR production of ^{2}H is induced by particles with $E > 100$ MeV. The calculated production rates for ^{2}H are 8.0-9.5 times those for tritium. Because ^{3}H production rates are under-calculated by a factor of 1.4 (Reedy, 1977), the calculated ^{2}H production rates would have been expected to be lower than the observed rates. Perhaps the $^{2}H/^{3}H$ production ratios adopted here are too high, or the excitation functions for producing ^{2}H and ^{3}H have different shapes.

COSMOGENIC FISSION OF URANIUM AND THORIUM

Cosmic-ray particles, especially secondary neutrons, can induce the fission of ^{232}Th, ^{235}U, and ^{238}U. The resulting fission products are sources both of nuclides, like ^{136}Xe, and of fossil charged-particle tracks. The spontaneous fission of ^{238}U (which has a partial half-life of 8.2×10^{15} years) is the source of most fission in lunar samples, occurring at a rate of 404 fissions/min/kg-U. Because the cross sections for cosmic-ray-induced fission of Th and U isotopes are high (~1 barn), rates for cosmogenic fission are similar to those for spontaneous fission. In samples with long exposures to the cosmic rays (e.g. lunar cores), cosmogenic fission could be a significant fraction of the fissions which have occurred (Damm et al., 1978). As noted by K. Marti (priv. comm., 1980), certain nuclides, like ^{136}Xe and ^{86}Kr, are made at relatively low rates by spallation reactions (Hohenberg et al., 1978; Regnier et al., 1979), but in high yields by fission reactions; so cosmogenic fission could be an important source of these nuclides in lunar samples. To study quantitatively the importance of cosmogenic fission in lunar samples, fission cross sections were evaluated and used to calculate rates for the fission of Th and U isotopes by GCR particles and by solar protons. Damm et al. (1978) calculated rates for the fission of U, Th, Bi, Pb, and Au by GCR particles in the moon, but used (p,f) cross sections. Their results showed that the fission of Bi, Pb, and Au are relatively unimportant in lunar samples compared to the fission of U and Th.

The cross sections for the fission of ^{232}Th, ^{235}U, and ^{238}U by galactic-cosmic-ray particles were adopted or estimated from a number of sources. For neutrons with E < 40 MeV, the fission cross sections compiled in BNL-325 (Garber and Kinsey, 1976) were used. For protons with E > 100 MeV, the cross sections summarized in de Carvalho et al. (1962) and Friedlander (1965) were used. In the preliminary calculations reported in Reedy (1981), the fission cross sections were assumed to remain constant for E > 400 MeV. Above ~400 MeV, the product nuclides with 50 < A < 170, which can be made only by fission reactions at lower energies, can be produced by other types of reactions. Although the total production cross sections for nuclides with 50 < A < 170 remains constant for E > 200 MeV, the cross sections for binary fission decrease for energies above ~100 MeV (Friedlander, 1965). The shape of the excitation functions for proton-induced fission for 40 < E < 100 MeV was estimated from the cross sections for several fission products made by the $^{238}U(p,f)$ reaction (Diksic et al., 1974). There is an appreciable flux of neutrons for E ~ 50 MeV, so the fission cross sections from 40 to about 60 MeV were increased above the proton-induced values because, at 30 MeV, cross sections for neutron-induced fission are higher than those for proton-induced fission. Because of the scarcity of measured total fission cross sections for 30 < E < 100 MeV, especially with neutrons, there are considerable uncertainties in the cross sections adopted for this energy region. In particular, the U(n,f) cross sections for 30 to 40 MeV (Garber and Kinsey, 1976), which are used here, seem too high.

The excitation functions for proton-induced fission of natural uranium and thorium at low energies were based on the cross sections measured by Boyce et al. (1974) for U(p,f) with E_p < 30 MeV and by Choppin et al. (1963) and Eaker and Choppin (1976) for Th(p,f) with E_p < 16 MeV. Cross sections summarized in de Carvalho et al. (1963) were used to connect these low-energy data with the adopted GCR cross sections at 100 MeV. These (p,f) excitation functions are very similar to those of Damm et al. (1978). When these (p,f) cross sections were used to calculate fission rates of U and Th by GCR particles, the results agreed within about 2% or less with the calculated production rates of Damm et al. (1978). The cross sections for (p,f) reactions are lower than those for (n,f) reactions with Th and U for energies below about 18 and 100 MeV, respectively. For the lunar GCR-particle spectrum, the GCR cross-section set for U gave fission rates higher than those calculated with the U(p,f) excitation function by factors of 1.87 and 1.39 for 10 < E < 30 MeV and 30 < E < 100 MeV, respectively.

The excitation functions for the production of ^{86}Kr, ^{134}Xe, and ^{136}Xe from ^{232}Th, ^{235}U, and ^{238}U by GCR particles were constructed from evaluated fission yields and the adopted fission cross sections for E < 20 MeV and from measured cross sections for producing these nuclides at energies above 60 MeV. Cross sections for other fission products were not constructed because such nuclides are made in high yields by other cosmogenic nuclear reactions (e.g., ^{131}Xe) or are naturally present in samples (e.g., barium isotopes). All radioactive fission products with these masses which decay to these three nuclides (e.g., ^{136}Te and ^{136}I for ^{136}Xe) were included, and fission products which decayed to other stable isotopes (e.g., ^{136}Cs, which decays to ^{136}Ba) were excluded. The evaluated fission yields of Rider and Meek (1978) were used for fission-spectrum (~1 MeV) and 14-MeV neutrons and linearly interpolated for $1 < E < 14$ MeV. For $E > 60$ MeV, cross sections for the fission products which decay to these three nuclides were determined from a large number of cumulative or independent cross sections. The cross sections for the production of noble-gas nuclides as measured by Regnier (1977) for Th(p,f) reactions at 0.15 and 1.05 GeV, by Hudis et al. (1970) for U(p,f) reactions at 3 and 29 GeV, and by Yu et al. (1973) for the U(p,f) reaction at 11.5 GeV were used. For the production of ^{134}Xe by ^{238}U(p,f) reactions, the total cross sections for producing the mass-134 chain, less the independent cross sections for making isotopes which decayed to ^{134}Ba (such as ^{134}Cs and ^{134}La), were used. Smooth trends in cross sections or isotope ratios (e.g., $^{134}Cs/^{134}Xe$) versus energy were used when no experimental data were available. Cross sections for the other eight target-product combinations were determined similarly. For $15 < E < 60$ MeV, product yields were interpolated from the measured 14-MeV yields and yields inferred from the cross sections for these products and for fission at $E \cong 60$ MeV. Separate excitation functions for each target-product combination had to be determined because the yields of most fission products per fission vary with energy (see, e.g., Friedlander, 1965). For example, the cumulative yield of ^{136}Xe per fission of ^{238}U varies from 6.85% for ~1-MeV neutrons to 0.8% for 1-GeV protons. These excitation functions are different than those used in the preliminary calculations reported by Reedy (1981).

The excitation functions used for the production of ^{134}Xe and ^{136}Xe by (p,f) reactions below 100 MeV were based mainly on measured cross sections. Estimated yields were used at many energies to get ^{86}Kr production cross sections, so the calculated solar-proton production rates for ^{86}Kr have greater uncertainties than those for other fission reactions. For the production of all three of these nuclides by the Th(p,f) reaction at 15.6 MeV, the cross sections of Eaker and Choppin (1976) were used. The excitation functions for the production of ^{134}Xe and ^{136}Xe by Th(p,f) reactions for 25 < E < 87 MeV were based on the measured cross sections of Pate _et al_. (1958). The Th(p,f)^{86}Kr cross sections for energies between 15.6 and 150 MeV and for E < 15.6 MeV were estimated by assuming that the yield of ^{86}Kr per fission varied slowly with energy. The cross sections for the production of ^{134}Xe and ^{136}Xe by the U(p,f) reaction were based mainly on the measurements of Diksic _et al_. (1974). The U(p,f)^{86}Kr excitation function below 100 MeV was constructed by assuming fission yields of about 1.25% for E > 50 MeV and 0.3-0.4% for E < 40 MeV.

The rates for the fission or the production of ^{86}Kr, ^{134}Xe, and ^{136}Xe from Th and natural uranium were calculated using the lunar GCR fluxes of Reedy and Arnold (1972) and are given in Table 1. Only particles with E ≳ 0.2 MeV were considered, as the Reedy-Arnold GCR-particle-flux model is good only for E > 0.5 MeV. Relatively few fission reactions occur for particles having energies between 0.2 and 0.5 MeV. Only ^{235}U can be fissioned by particles with E < 0.2 MeV, and the rates for the $^{235}U(n,f)$ reaction as a function of depth were determined from the Lunar Neutron Probe Experiment (LNPE) by Woolum and Burnett (1974). Because natural uranium consists of only 0.72% ^{235}U, almost all (≅99%) of the fissions induced in U by particles with E ≳ 0.2 MeV are from ^{238}U. The average yields of ^{86}Kr, ^{134}Xe, and ^{136}Xe per fission usually increased with depth because of the increased ratio of secondary neutrons to high-energy particles. The ratios for $^{134}Xe/^{136}Xe$ production rates decreased less than 10% with depth, but the $^{86}Kr/^{136}Xe$ production ratios decreased with depth by factors of 1.33 and 1.73 for Th and U, respectively.

The total fission rates calculated here are higher than those calculated by Damm et al. (1978) because of the higher cross sections used here for energies below 18 and 100 MeV for the fission of Th and U, respectively (see above in paragraph on proton-induced fission cross sections). For natural uranium, the fission rates given in Table 1 for the lunar surface and a depth of 225 g/cm^2 are higher than those of Damm et al. (1978) by factors of 1.29 and 1.85, respectively. Because 40% (at the lunar surface) to 84% (depths below 500 g/cm^2) of the cosmogenic fissions of ^{238}U are induced by particles with $E < 100$ MeV, the differences in the GCR and (p,f) excitation functions can account for these differences in calculated production rates. At depths of 0 and 225 g/cm^2, the rates calculated here for the fission of Th are 1.04 and 1.23 times those of Damm et al. (1978). This difference is due mainly to fission of Th induced by particles with $E < 15$ MeV.

The cosmogenic fission rates calculated here or determined from the LNPE data by Woolum and Burnett (1974) are compared with the rate for the spontaneous fission of ^{238}U in Fig. 1, assuming the lunar Th/U ratio of 3.8 and the present ^{235}U isotopic abundance of 0.72%. The $^{235}U(n,f)$ rates are from the smooth curve in Fig. 4 of Woolum and Burnett (1974). Their results should be divided by a factor of 1.21 to convert the rates measured by the LNPE during the Apollo-17 mission to those averaged over a solar cycle (Woolum and Burnett, 1974). However, the Apollo 17 soil into which the LNPE was placed had a high macroscopic cross section, Σ, for neutron capture (0.00936 cm^2/g) because of its high concentrations of Fe and Ti. Rates for neutron-capture reactions vary with Σ, and the rate for the $^{235}U(n,f)$ reaction would increase by a factor of 1.21 for a more typical Σ of 0.0075 cm^2/g (Reedy, 1978). Thus, the uncorrected LNPE rates would apply for a solar-cycle averaged rate in a typical lunar soil. At these depths, and other lunar depths above 200 g/cm^2, the total rates for the cosmogenic fission of ^{232}Th, ^{235}U, and ^{238}U are ≅12 times the rate for the spontaneous fission of ^{238}U. A similar ratio for cosmogenic to spontaneous fission rates was calculated by Damm _et al_. (1978). Thus cosmic-ray-induced reactions can produce a significant fraction of the total number of fissions that have occurred in lunar samples with long (~10^8 years or more) exposure ages, so cosmogenic fission must be considered in studies involving fission-track dating, ^{244}Pu fission, and fission products.

In discussing the origins of fossil charged-particle tracks in meteorites, Fleischer _et al_. (1967) noted that there are two types of cosmogenic fission tracks. Fission induced by high-energy ("energies greater than ~100 MeV") particles produces V-shaped tracks because of the large momentum of the incident projectile. Fission induced by low-energy particles produces linear tracks like those made by spontaneous fission. The fractions of fissions induced by particles with E > 100 MeV range from 70% to 24% for Th and from 60% to 15% for ^{238}U. Almost all of the fission of ^{235}U is induced by low-energy neutrons. At lunar depths of 40 and 225 g/cm^2, 30% and 18% of the total fisions of ^{232}Th, ^{235}U, and ^{238}U are induced by particles with E > 100 MeV; and 4.6% and 1.0%, respectively, of the fissions at these two depths are induced by particles with E > 1 GeV. As noted by Fleischer _et al_. (1967), the densities of cosmogenic fission tracks vary with depth, and the V-shaped tracks decrease in density more rapidly with greater depths than do the other cosmogenic fission tracks.

Because the half-lives of these three fissile nuclides are about the same as the age of the moon but are different (^{232}Th = 1.40 x 10^{10} years, ^{235}U = 7.04 x 10^8 years, and ^{238}U = 4.47 x 10^9 years), the ratios of their fission rates were different during the early history of the moon. In particular, the rates for the ^{235}U(n,f) reaction >10^9 years ago were relatively much greater than those for the fission of ^{232}Th or ^{238}U. Eugster _et al_. (1979) observed excess ^{136}Xe in the soils of the 74001/2 cores which they concluded was produced by the $^{235}U(n,f)$ reaction about 3.8×10^9 years ago. As noted above, the rates for the $^{235}U(n,f)$ reaction also change with neutron macroscopic cross section.

The yields of ^{136}Xe, ^{134}Xe, and ^{86}Kr per cosmogenic fission varied with depth and were different from their yields by the spontaneous fission of ^{238}U. The yields of ^{136}Xe, ^{134}Xe, and ^{86}Kr per cosmogenic fission of ^{232}Th and ^{238}U were ~0.4, ~0.6, and ~2-3, respectively, of their yields for the spontaneous fission of ^{238}U (6.4, 5.3, and 0.9%, respectively). Thus, as with total fission, cosmogenic fission could produce significant amounts of these three fission products (especially ^{86}Kr). The production of other Kr and Xe isotopes by cosmic-ray-induced fission also could be relatively important because, like ^{86}Kr, these nuclides are produced in greater yields by cosmogenic fission than they are by the spontaneous fission of ^{238}U.

These three noble-gas nuclides are made in relatively low yields by spallation reactions and ^{86}Kr and ^{134}Xe are more abundant in lunar rocks than calculated for spallation reactions (Hohenberg _et_ _al_., 1978; Regnier _et_ _al_., 1979). The average lunar composition of Reedy (1978) was used to compare the production rates for these three nuclides by spallation reactions and by cosmogenic fission of ^{232}Th and ^{238}U. At the lunar surface and below 500 g/cm^2, the fission/spallation production ratios were 0.12-0.38 for ^{86}Kr, 0.13-1.15 for ^{134}Xe, and 0.9-7.1 for ^{136}Xe. The $^{235}U(n,f)$ reaction was not included, but would increase these ratios, especially at depths below ~100 g/cm^2. Therefore, cosmogenic fission cannot account for the undercalculation of cosmogenic ^{86}Kr and ^{134}Xe in lunar rocks, but is an important source of cosmic-ray-produced ^{136}Xe. (The undercalculation of ^{86}Kr and ^{134}Xe production rates for spallation reactions probably is caused by low estimated cross sections for their production from Zr and rare earth elements.)

DISCUSSION

The production rates reported here were for a variety of reactions, and most reactions have not had their production rates published elsewhere. Production rates for ^{3}He, ^{15}N, ^{13}C, and ^{2}H previously had been inferred from their measured concentrations and experimentally determined exposure ages. The production rates c[illegible]ulated here for these nuclides agreed with the inferred values within fact[illegible] .5, quite good agreement considering the uncertainties in both the exper[illegible]ental results and/or in the excitation functions used in these calculations. For the reactions studied here, the production-rate-versus-depth profiles probably are calculated very well. Erosion of rock surfaces or gardening of the lunar soil will modify these production profiles, especially for the solar-proton-induced reactions and for samples with long (~10^{7} years or more) exposure ages.

The ^{3}He production rates calculated here, multiplied by 1.4 for GCR-induced reactions, can be used to predict the concentrations of cosmogenic ^{3}He in studies of ^{3}He in lunar samples. Solar-proton-induced reactions with bromine should produce only a small fraction of the ^{78}Kr, ^{80}Kr, and ^{81}Kr observed in lunar samples. The $^{130}Ba(n,p)$ reaction produces ~1% of the ^{130}Xe made from barium; thus the reason that the ^{130}Xe production rate is undercalculated in lunar samples by Hohenberg et al. (1978) is not known. The calculated production rates of ^{15}N (actually about 1.5 times the ^{15}O values), ^{13}C, and ^{2}H agree approximately with the measured data for these isotopes in lunar samples with long exposure ages, confirming that cosmic-ray-induced reactions can account for most of the excesses of these isotopes observed in such lunar samples. The contemporary fluxes of cosmic-ray particles would produce ≅0.5% of the excess ^{15}N observed in the atmosphere of Mars.

The rates for the fission of U and Th by cosmic-ray particles within 200 g/cm^2 of the lunar surface are ≅12 times the rate for the spontaneous fission of ^{238}U. The productions of ^{86}Kr and ^{134}Xe by cosmogenic fission are important sources of these nuclides, and cosmogenic fission produces more ^{136}Xe than do spallation reactions with Ba and rare earth elements. Rates for the $^{235}U(n,f)$ reaction vary with the chemical composition, and would be relatively more important, compared to fission of ^{232}Th and ^{238}U, more than ~10^9 years ago. Cosmogenic fission of Th and U can be important sources of fission tracks or fission-product nuclides, especially in samples with long exposure ages.

ACKNOWLEDGMENTS

This work was supported by NASA under work order W-14,084 and done under the auspices of the U. S. Department of Energy. The author thanks K. Marti for suggesting some of the reactions studied in this work and L. M. Mitchell, C. Gallegos, and M. L. Ennis for their help in preparing the manuscript.

REFERENCES

Albouy M. G., Cohen J.-P., Gusakow M., Poffe N., Sergolle H., and Valentin L. (1962) Spallation de l'oxygene par des protons de 20 à 150 MeV. Phys. Lett. 2, 306-307.

Armstrong T. W. and Alsmiller R. G. (1971) Calculation of cosmogenic radionuclides in the Moon and comparison with Apollo measurements. Proc. Lunar Sci. Conf. 2nd, p. 1729-1745.

Audouze J., Epherre M., and Reeves H. (1967) Survey of experimental cross sections for proton-induced spallation reactions in He^4, C^{12}, N^{14}, and O^{16}. In High-Energy Nuclear Reactions in Astrophysics (B. S. P. Shen, ed.), p. 255-271. W. A. Benjamin, New York.

Badhwar G. D. and Daniels R. R. (1963) Some remarks concerning the energy dependence of the intensities of nuclei of helium-3, lithium, beryllium, and boron in the galactic cosmic radiation. Progr. Theor. Phys. 30, 615-626.

Becker R. H., Clayton, R. N., and Mayeda T. K. (1976) Characterization of lunar nitrogen components. Proc. Lunar Sci. Conf. 7th, p. 441-458.

Bertrand F. E. and Peelle R. W. (1973) Complete hydrogen and helium particle spectra from 30- to 60-MeV proton bombardment of nuclei with A=12 to 209 and comparison with the intranuclear cascade model. Phys. Rev. C 8, 1045-1064.

Birattari C., Gadioli E., Gadioli Erda E., Grassi Strini A. M., Strini G., and Tagliaferri G. (1973) Pre-equilibrium processes in (p,n) reactions. Nucl. Phys. A201, 579-592.

Boyce J. R., Hayward T. D., Bass R., Newson H. W., Bilpuch E. G., Purser F. O., and Schmitt H. W. (1974) Absolute cross sections for proton-induced fission of the uranium isotopes. Phys. Rev. C 10, 231-244.

Brill' O. D., Vlasov N. A., Kalinin S. P., and Sokolov L. S. (1961) Cross section of the (n,2n) reaction in C^{12}, N^{14}, O^{16}, and F^{19} in the energy interval 10-37 MeV. Dokl. Akad. Nauk SSSR 136, 55-57; also in Sov. Phys. Dokl. 6, 24-26.

Choppin G. R., Meriwether J. R., and Fox J. D. (1963) Low-energy charged-particle-induced fission. Phys. Rev. 131, 2149-2152.

Collé R. and Kishore R. (1974) Excitation functions for (p,n) reactions on ^{79}Br and ^{127}I. Phys. Rev. C 9, 2166-2170.

Cressy P. J. and Bogard D. D. (1976) On the calculation of cosmic-ray exposure ages of stone meteorites. Geochim. Cosmochim. Acta 40, 749-762.

Damm G., Thiel K., and Herr W. (1978) Cosmic-ray-induced fission of heavy nuclides: Possible influence on apparent ^{238}U-fission track ages of extraterrestrial samples. Earth Planet. Sci. Lett. 40, 439-444.

de Carvalho H. G., Cortini G., Muchnik M., Potenza G., and Rinzivillo R. (1963) Fission of uranium, thorium and bismuth by 20 GeV protons. Nuovo Cim. 27, 468-474.

Des Marais D. J. (1978) Carbon, nitrogen, and sulfur in Apollo 15, 16, and 17 rocks. Proc. Lunar Planet. Sci. Conf. 9th, p. 2451-2467.

Des Marais D. J. (1980) Six lunar rocks have little carbon and nitrogen and some rocks have detectible spallogenic ^{13}C (abstract). In Lunar and Planetary Science XI, p. 228-230. Lunar and Planetary Institute, Houston.

Diksic M., McMillan D. K., and Yaffe L. (1974) Nuclear charge dispersion in mass chains 130-135 from the fission of ^{238}U by medium-energy protons. J. Inorg Nucl. Chem. 36, 7-16.

Eaker R. W. and Choppin G. R. (1976) Mass and charge distribution in the fission of ^{232}Th. J. Inorg. Nucl. Chem. 38, 31-36.

Eberhardt P., Geiss J., and Graf H. (1971) On the origin of excess ^{131}Xe in lunar rocks. Earth Planet. Sci. Lett. 12, 260-262.

Epstein S. and Taylor H. P. (1971) O^{18}/O^{16}, Si^{30}/Si^{28}, D/H, and C^{13}/C^{12} ratios in lunar samples. Proc. Lunar Sci. Conf. 2nd, p. 1421-1441.

Eugster O., Grögler N., Eberhardt P., and Geiss J. (1979) Double drive tube 74001/2: History of the black and orange glass; determination of a pre-exposure 3.7 AE ago by $^{136}Xe/^{235}U$ dating. Proc. Lunar Planet. Sci. Conf. 10th, p. 1351-1379.

Fleischer R. L., Price P. B., Walker R. M., and Maurette M. (1967) Origins of fossil charged-particle tracks in meteorites. *J. Geophys. Res.* *72*, 331-353.

Foster D. G. and Young P. G. (1972) A preliminary evaluation of the neutron and photon-production cross sections of oxygen. AEC report LA-4780. 30 pp.

Friedlander G. (1965) Fission of heavy elements by high-energy protons. In *Physics and Chemistry of Fission*, Vol. II, p 265-282. IAEA, Vienna.

Friedman I., O'Neil J. R., Gleason J. D., and Hardcastle K. (1971) The carbon and hydrogen content and isotopic composition of some Apollo 12 materials. *Proc. Lunar Sci. Conf.* *2nd*, pp. 1407-1415.

Fulmer C. B. and Goodman C. D. (1960) (p,α) reactions induced by protons in the energy range of 9.5-23 MeV. *Phys. Rev.* *117*, 1339-1344.

Garber D. I. and Kinsey R. R. (1976) Neutron cross sections volume II, curves. ERDA report BNL-325, 3rd edition, Vol. II, 491 pp.

Goebel K., Schultes H., and Zaehringer J. (1964) Production cross sections of tritium and rare gases in various target elements. CERN report CERN-64-12. 78 pp.

Hohenberg C. M., Marti K., Podosek F. A., Reedy R. C., and Shirck J. R. (1978 Comparisons between observed and predicted cosmogenic noble gases in lunar samples. *Proc. Lunar Planet. Sci. Conf.* *9th*, p. 2311-2344.

Hudis J., Kirsten T., Stoenner R. W., and Schaeffer O. A. (1970) Yields of stable and radioactive rare-gas isotopes formed by 3- and 29-GeV proton bombardment of Cu, Ag, Au, and U. Phys. Rev. C 1, 2019-2030.

Kaiser W. A. (1977) The excitation function of Ba(p,X)^{M}Xe (M = 124-136) in the energy range 38-600 MeV; the use of 'cosmogenic' xenon for estimating 'burial' depths and 'real' exposure ages. Phil. Trans. R. Soc. Lond. A. 285, 337-362.

Kaiser W. A. and Berman B. L. (1972) The average ^{130}Ba(n,γ) cross section and the origin of ^{131}Xe on the moon. Earth Planet. Sci. Lett. 15, 320-324.

Kohl C. P., Murrell M. T., Russ G. P., and Arnold J. R. (1978) Evidence for the constancy of the solar cosmic ray flux over the past ten million years: ^{53}Mn and ^{26}Al measurements. Proc. Lunar Planet. Sci. Conf. 9th, p. 2299-2310.

Kruger S. T. and Heymann D. (1973) High-energy proton production of ^{3}H, ^{3}He, and ^{4}He in light targets. Phys. Rev. C 7, 2179-2187.

Kumabe I., Ogata H., Komatuzaki T., Inoue N., Tomita S., Yamada Y., Yamaki T., and Matsumoto S. (1963) (p,α) reactions on the even nuclei Ni^{58}, Ni^{60} and Fe^{56}. Nucl. Phys. 46, 437-453.

Merlivat L., Lelu M., Nief G., and Roth E. (1974) Deuterium, hydrogen, and water content of lunar material. Proc. Lunar Sci. Conf. 5th, p. 1885-1895.

Merlivat L., Lelu M., Nief G., and Roth E. (1976) Spallation deuterium in rock 70215. Proc. Lunar Sci. Conf. 7th, p. 649-658.

Müller O., Hampel W., Kirsten T., and Herzog G. F. (1981) Cosmic-ray constancy and cosmogenic production rates in short-lived chondrites. Geochim. Cosmochim. Acta 45, 447-460.

Nishiizumi K., Regnier S., and Marti K. (1980) Cosmic ray exposure ages of chondrites, pre-irradiation and constancy of cosmic ray flux in the past. Earth Planet. Sci. Lett. 50, 156-170.

Owens T., Biemann K., Rushneck D. R., Biller J. E., Howarth D. W., and Lafleur A. L. (1977) The composition of the atmosphere at the surface of Mars. J. Geophys. Res. 82, 4635-4639.

Pate B. D., Foster J. S., and Yaffe L. (1958) Distribution of nuclear charge in the proton-induced fission of Th^{232}. Can. J. Chem. 36, 1691-1706.

Pulfer P. (1979) Bestimmung von absoluten produktionsquerschnitten fuer protonen-induzierte reaktionen im energiebereich zwischen 15 MeV und 72 MeV und bei 1820 MeV. Modellrechnungen fuer die produktion von Ne20, Ne21 und Ne22 an der mondoberflaeche durch die bestrahlung mit solaren protonen. Thesis, Univ. Bern. 150 pp.

Rao M. N. and Venkatesan T. R. (1980) Solar-flare produced ^3He in lunar samples. Nature 286, 788-790.

Reedy R. C. (1977) Solar proton fluxes since 1956. Proc. Lunar Sci. Conf. 8th, p. 825-839.

Reedy R. C. (1978) Planetary gamma-ray spectroscopy. Proc. Lunar Planet. Sci. Conf. 9th, p. 2961-2984.

Reedy R. C. (1980) Lunar radionuclide records of average solar-cosmic-ray fluxes over the last ten million years. Proc. Conf. Ancient Sun, p. 365-386.

Reedy R. C. (1981) Cosmic-ray-produced stable nuclides: Various production rates and their implications (abstract). In Lunar and Planetary Science XII, p. 871-873. Lunar and Planetary Institute, Houston.

Reedy R. C. and Arnold J. R. (1972) Interaction of solar and galactic cosmic-ray particles with the moon. J. Geophys. Res. 77, 537-555.

Reedy R. C., Herzog G. F., and Jessberger E. K. (1978) Depth variations of spallogenic nuclides in meteorites (abstract). In Lunar and Planetary Science IX, p. 940-942. Lunar and Planetary Institute, Houston.

Reedy R. C., Herzog G. F., and Jessberger E. K. (1979) The reaction Mg(n,α)Ne at 14.1 and 14.7 MeV: Cross sections and implications for meteorites. Earth Planet. Sci. Lett. 44, 341-348.

Regnier S. (1977) Production des gaz rares Ne, Ar, Kr et Xe au cours des réactions nucléaires induites par des protons de haute énergie dans des cibles allant de ^{27}Al à ^{232}Th. Thesis, Univ. de Bordeaux I. 106 pp.

Regnier S., Hohenberg C. M., Marti K., and Reedy R. C. (1979) Predicted versus observed cosmic-ray-produced noble gases in lunar samples: Improved Kr production ratios. Proc. Lunar Planet. Sci. Conf. 10th, p. 1565-1586.

Rider B. F. and Meek M. E. (1978) Compilation of fission product yields. General Electric Co., Vallecitos Nuclear Center report NEDO-12154-2(E).

Schultz L. and Signer P. (1976) Depth dependence of spallogenic helium, neon, and argon in the St. Severin chondrite. Earth Planet. Sci. Lett. **30**, 191-199.

Shapiro M. M. and Silberberg R. (1970) Heavy cosmic ray nuclei. Ann. Rev. Nucl. Sci. **20**, 323-392.

Sherr R. and Brady F. P. (1961) Spectra of (p,α) and (p,p') reactions and the evaporation model. Phys. Rev. **124**, 1928-1943.

Signer P. and Nier A. O. C. (1962) The measurement and interpretation of rare gas concentrations in iron meteorites. In Researches on Meteorites (C. B. Moore, ed.), p. 7-35. John Wiley & Sons, New York.

Venkatesan T. R., Nautiyal C. M., Padia J. T., and Rao M. N. (1980) Solar (flare) cosmic ray proton fluxes in the recent past. Proc. Lunar Planet. Sci. Conf. 11th, p. 1271-1284.

Walton J. R., Heymann D., Yaniv A., Edgerley D., and Rowe M. W. (1976a) Cross sections for He and Ne isotopes in natural Mg, Al, and Si, He isotopes in CaF_2, Ar isotopes in natural Ca, and radionuclides in natural Al, Si, Ti, Cr, and stainless steel induced by 12- to 45-MeV protons. J. Geophys. Res. **81**, 5689-5699.

Walton J. R., Heymann D., and Yaniv A. (1976b) Production of He, Ne, and Ar isotopes and U^{236} in lunar materials by solar cosmic ray protons -- production rate calculations. J. Geophys. Res. 81, 5701-5710.

Woolum D. S. and Burnett D. S. (1974) In-situ measurement of the rate of ^{235}U fission induced by lunar neutrons. Earth Planet. Sci. Lett. 21, 153-164.

Yanagita S. and Imamura M. (1978) Excess ^{15}N in the martian atmosphere and cosmic rays in the early solar system. Nature 274, 234-235.

Yaniv A. and Kirsten T. (1981) Isotopic ratios of rare gases and the role of nuclear reactions in solar flares (abstract). In Lunar and Planetary Science XII, p. 1224-1226. Lunar and Planetary Institute, Houston.

Yu Y. W., Porile N. T., Warasila R., and Schaeffer O. A. (1973) Cross sections and recoil properties of xenon isotopes formed in 11.5-GeV proton bombardment of ^{238}U. Phys. Rev. C 8, 1091-1098.

Table 1

GCR production rates (per minute per kg-element)
versus depth for particles with E ≥0.2 MeV.

Depths (g/cm^2) Product	Target	0	5	10	20	40	65	100	150	225	350	500
^{2}H	O	1949	1984	2016	2037	1925	1700	1358	991	634	294	91
^{2}H	Mg	1005	995	987	964	875	749	582	410	251	110	34
^{2}H	Al	900	890	884	864	784	672	523	370	227	100	31
^{2}H	Si	870	861	854	835	757	648	504	355	217	96	29
^{2}H	Fe	409	395	383	363	316	262	198	134	78	32	9.6
^{3}He	O	438	441	444	442	409	354	278	198	122	54	16.3
^{3}He	Mg	314	317	320	321	302	266	213	155	100	47	14.4
^{3}He	Al	292	294	297	298	280	246	196	143	91	43	13.2
^{3}He	Si	301	304	306	307	287	252	201	146	93	43	13.3
^{3}He	Fe	154	150	147	141	126	106	81	57	34	14.6	4.4
^{4}He	O	2698	2928	3148	3447	3600	3434	2940	2331	1659	873	281
^{4}He	Mg	1756	1938	2114	2357	2513	2432	2108	1694	1224	655	212
^{4}He	Al	1606	1746	1880	2063	2159	2063	1769	1405	1002	529	170
^{4}He	Si	1530	1658	1782	1949	2032	1937	1657	1312	933	[illegible]	158
^{4}He	Fe	825	861	896	940	936	863	718	552	379	192	61
^{13}C	O	360	442	521	640	755	782	716	610	471	271	89
^{15}O	O	369	407	442	491	519	500	431	343	246	130	41.9
Fission	Th	523	589	653	742	807	791	693	563	412	223	72.4
Fission	U	1000	1158	1311	1534	1721	1725	1539	1276	957	533	174
^{86}Kr	Th	17.0	19.8	22.5	26.5	30.0	30.2	27.1	22.6	17.1	9.6	3.1
^{86}Kr	U	14.0	16.2	18.3	21.5	24.2	24.2	21.7	18.0	13.5	7.5	2.5
^{134}Xe	Th	11.4	13.7	16.0	19.4	22.5	23.1	21.0	17.7	13.6	7.7	2.5
^{134}Xe	U	32.0	40.4	48.6	60.9	73.1	76.4	70.4	60.3	46.8	27.0	8.9
^{136}Xe	Th	9.4	11.5	13.6	16.7	19.7	20.3	18.6	15.8	12.2	7.0	2.3
^{136}Xe	U	22.4	28.9	35.2	44.7	54.3	57.2	52.9	45.6	35.7	20.7	6.9

Table 2

Solar-proton production rates (per minute per kg-element) versus depth using R_o = 100 MV and $J(4\pi, E>10\ MeV)$ = 100 protons/cm^2s.

Depths (g/cm^2)		0	0.07	0.15	0.325	0.70	1.50	3.20	7.00	15.0	30.0
Product	Target										
^{2}H	O	3976	3454	3108	2623	2038	1430	894	483	242	149
^{2}H	Mg	[illegible]	954	878	765	618	453	295	166	85	53.3
^{2}H	Al	1091	965	878	753	597	429	275	153	78	48.6
^{2}H	Si	938	841	772	670	540	394	256	144	74	46.2
^{2}H	Fe	286	245	219	185	145	104	68	38.5	20.3	12.9
^{3}He	O	495	450	417	367	300	223	148	84.8	44.5	28.0
^{3}He	Mg	641	569	518	443	348	246	154	82.5	40.7	24.8
^{3}He	Al	610	538	487	415	325	229	143	76.8	38.0	23.2
^{3}He	Si	550	492	449	387	307	220	139	75.5	37.6	23.0
^{3}He	Fe	144	127	116	99	79	57	36.6	20.4	10.5	6.6
^{4}He	O	24378	18876	15904	12295	8600	5378	2985	1433	648	378
^{4}He	Mg	17463	13844	11802	9244	6539	4110	2276	1082	482	279
^{4}He	Al	14463	10932	9173	7085	4970	3123	1742	841	381	223
^{4}He	Si	10984	8914	7697	6131	4424	2845	1616	789	360	211
^{4}He	Fe	2684	2078	1767	1394	1008	662	391	201	97	59
^{13}C	O	1462	1136	962	752	538	349	203	103	48	28.5
^{15}O	O	3138	2712	2418	2002	1499	989	566	273	122	70.1
^{78}Kr	Br	4369	3144	2500	1755	1062	547	241	89.7	32.2	16.7
^{80}Kr	Br	5910	4213	3349	2363	1453	773	359	144	55.7	30.2
^{81}Kr	Br	3885	1643	1050	581	283	123	48.5	16.7	5.8	2.9
Fission	Th	4974	3950	3369	2640	1869	1177	655	313	141	82
Fission	U	7839	6205	5282	4130	2915	1831	1013	485	217	126
^{86}Kr	Th	141	111	94	73	50	31	16.8	7.8	3.4	1.9
^{86}Kr	U	53	45	40	33	25	17	10.2	5.2	2.4	1.4
^{134}Xe	Th	168	126	104	77	51	29	14.8	6.5	2.7	1.5
^{134}Xe	U	263	207	176	138	97	61	33.5	15.7	6.8	3.9
^{136}Xe	Th	185	136	111	80	52	29	14.2	6.0	2.4	1.3
^{136}Xe	U	196	150	125	96	67	41	22.1	10.2	4.3	2.5

Table 3

Solar-proton production rates (per minute per kg-element) versus depth using R_0 = 200 MV and $J(4\pi, E>10 \text{ MeV})$ = 100 protons/cm^2s.

Depths	(g/cm^2)	0	0.07	0.15	0.325	0.70	1.50	3.20	7.00	15.0	30.0
Product	Target										
^{2}H	O	7856	7428	7109	6620	5946	5106	4163	3179	2338	1860
^{2}H	Mg	2593	2490	2409	2277	2084	1828	1523	1187	868	713
^{2}H	Al	2460	2347	2261	2126	1934	1686	1398	1087	813	653
^{2}H	Si	2270	2177	2105	1988	1818	1594	1329	1037	777	625
^{2}H	Fe	677	644	621	586	537	475	403	323	249	204
^{3}He	O	1329	1283	1245	1183	1090	965	813	641	484	391
^{3}He	Mg	1276	1212	1162	1082	971	828	668	502	362	285
^{3}He	Al	1202	1139	1091	1015	910	777	628	473	342	270
^{3}He	Si	1161	1107	1064	996	898	773	628	476	347	274
^{3}He	Fe	338	325	312	294	269	236	197	155	117	95
^{4}He	O	28426	25004	22913	20097	16768	13241	9880	6886	4670	3551
^{4}He	Mg	20776	18436	16951	14902	12423	9753	7197	4938	3294	2479
^{4}He	Al	16671	14564	13342	11717	9802	7765	5811	4060	2758	2098
^{4}He	Si	14334	12933	12009	10703	9076	7272	5487	3855	2628	2002
^{4}He	Fe	3742	3367	3142	2835	2462	2046	1619	1204	867	682
^{13}C	O	1877	1673	1549	1381	1180	960	739	530	367	281
^{15}O	O	4484	4143	3889	3504	2990	2386	1772	1211	800	597
^{78}Kr	Br	3363	2661	2241	1763	1248	801	473	256	139	94
^{80}Kr	Br	4746	3786	3250	2587	1899	1290	822	490	293	208
^{81}Kr	Br	1980	1019	728	473	285	162	88	45.7	24.2	16.2
Fission	Th	5992	5328	4904	4319	3611	2847	2113	1460	901	741
Fission	U	9355	8301	7632	6712	5602	4410	3269	2257	1515	1145
^{86}Kr	Th	158	139	127	110	90	70	57	34	22.6	16.9
^{86}Kr	U	93	77	73	66	58	48	37	26	18.1	13.8
^{134}Xe	Th	160	135	120	101	79	58	40	26	16.8	12.4
^{134}Xe	U	300	265	243	212	175	136	98	65	42.3	31.2
^{136}Xe	Th	164	135	119	98	75	53	36	22	13.8	10.0
^{136}Xe	U	207	179	162	140	114	87	62	41	25.8	18.8

FIGURE CAPTION

Fig. 1. Calculated rates for the fission of ^{232}Th, ^{235}U, and ^{238}U by GCR particles as a function of depth are compared with the rate for the spontaneous fission of ^{238}U. The rates for the fission of ^{232}Th and ^{238}U are from Table 1; those for $^{235}U(n,f)$ are from Woolum and Burnett (1974). The lunar Th/U ratio of 3.8 and the contemporary ^{235}U abundance of 0.72% were assumed.

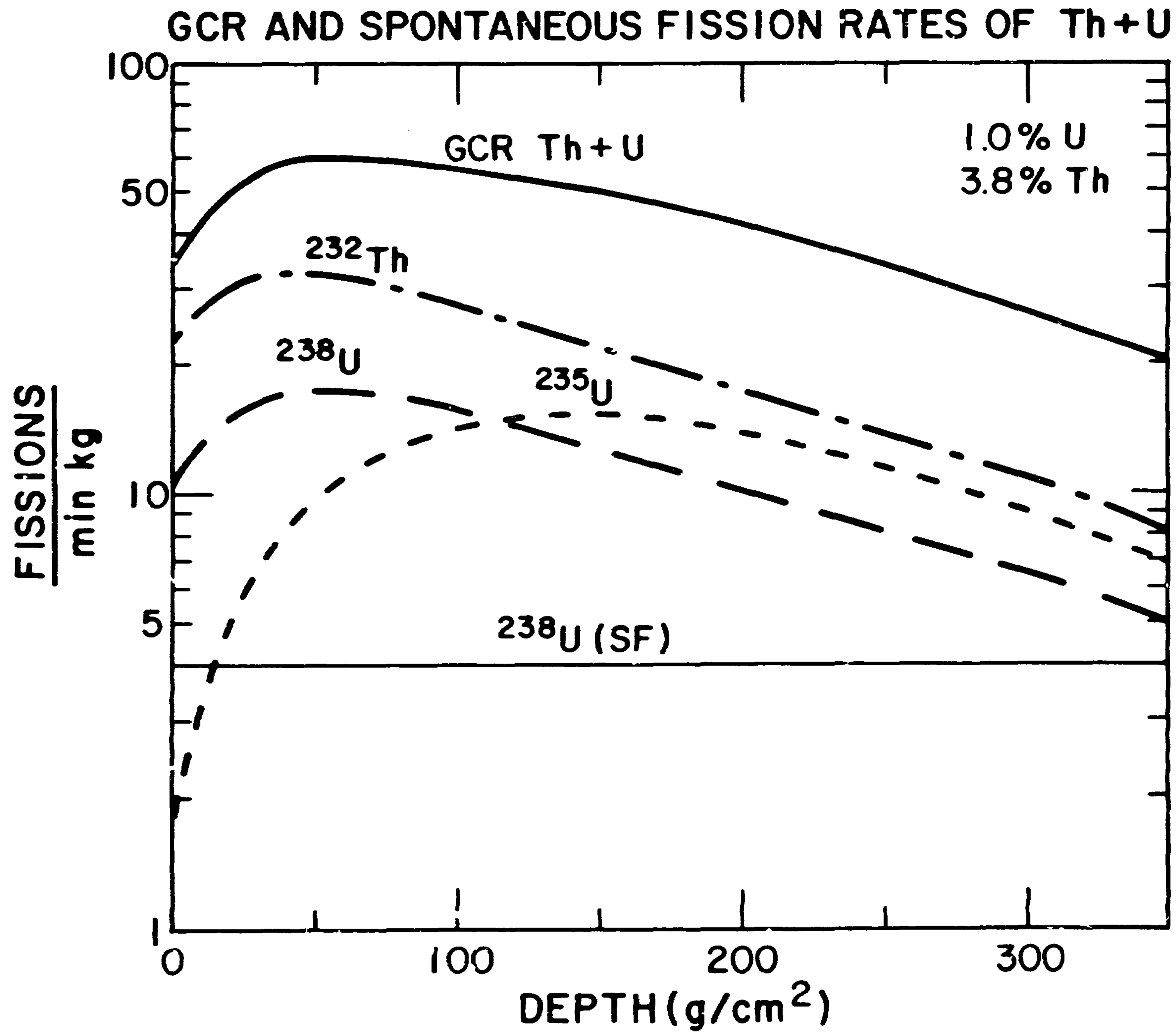

GCR AND SPONTANEOUS FISSION RATES OF Th+U
GCR Th+U
1.0% U
3.8% Th
232Th
238U
235U
238U (SF)
FISSIONS / min kg
DEPTH (g/cm2)
100
50
10
5
1
0
100
200
300